Modular Design of Picrosides Biosynthesis Unravelled Through Intermediates Flux Dynamics vis-à-vis Expression Analysis of Pathway Genes in a Medicinal Herb, *Picrorhiza kurroa* Royle ex Benth

SYNOPSIS

Submitted in fulfilment of the requirements for the degree of

Doctor of Philosophy

In

Biotechnology

By

VARUN KUMAR

Enrolment No. 126563

Under the supervision of

Prof. Rajinder Singh Chauhan

DEPARTMENT OF BIOTECHNOLOGY AND BIOINFORMATICS

JAYPEE UNIVERSITY OF INFORMATION TECHNOLOGY

WAKNAGHAT-173234, H.P., INDIA

DECEMBER 2016

Modular Design of Picrosides Biosynthesis Unravelled Through Intermediates Flux Dynamics vis-à-vis Expression Analysis of Pathway Genes in a Medicinal Herb, *Picrorhiza kurroa* Royle ex Benth

VARUN KUMAR

Introduction

Picrorhiza kurroa Royle ex Benth, locally known as Kutki, belongs to family Scrophulariaceae and is distributed at an elevation of 3000-5000 m above mean sea level in the North-Western Himalayas. It is used in the preparation of various herbal drug formulations viz. picroliv, katuki, arogya, livplus and livcare, due to pharmacological properties like hepatoprotective, antioxidant, anti-allergic, anti-asthmatic, anti-cancerous and immunomodulatory activity. It is used for the treatment of various liver ailments and consequently provide livelihood and health security to a large segment of high altitude populations. It is listed among top 15 most traded medicinal herbs in India with respect to revenues generated by traded material. *P. kurroa* is a self-propagating medicinal herb that originates as a young bud on stolons which develops to produce mature stolon and subsequently rhizomes with self-governing roots and shoots compartments [1]. Thus, during the collection of mature rhizomes of *P. kurroa*, all the young stolons and buds are also get uprooted which subsequently disrupt it's proliferation in natural habitat. The extensive harvesting has put this herb in the category of endangered medicinal herbs and thereby legal restrictions have been imposed on its collection from the wild [2]. The scarcity of raw material not only caused economic constraints on local communities but also resulted in adulteration of *P. kurroa* which has reduced its quality and efficacy due to lower levels of picroside-I (P-I) and picroside-II (P-II), the bioactive constituents of *P. kurroa* [2].

The picrosides, P-I and P-II, possess vast therapeutic activities as individual compounds and their bio-efficacy have also been tested via both *in vitro* as well as *in vivo* studies (Table 1).

Table 1. Bioactivities of P-I and P-II

Iridoid glycosides	Treatments	References
P-II	hind limb ischemia reperfusion injury	[3]
	anti-allergic asthma	[4]
	renal ischemia/reperfusion injury	[5]
	neuroprotective	[6-11]
	hepatoprotective	[12-13]
	hypoxia/reoxygenation induced cardiomyocyte injury	[14-15]
	myocardial ischemia reperfusion injury	[16]
P-I	hepatoprotective	[17]
	anti-cancer	[18]
P-I & P-II	Neuritogenesis	[19-20]

Moreover, the herbal drug formulations required both P-I and P-II in a ratio of 1:1.5 [2]. In *P. kurroa*, the accumulation of P-I and P-II are limited to specific tissues and regulated in response to alterations in environmental conditions. The stolons/rhizomes contained both P-I and P-II while only P-I is produced in shoots [1]. Moreover, 25°C temperature hinders the P-I accumulation whereas, 15°C increases its accumulation upto ~20-fold in *in vitro* grown *P. kurroa* shoots [21]. In contrast, P-II has not been produced in *P. kurroa* plants grown *in vitro*. Therefore, it is crucial to enable P-II access in shoots to protect rhizomes which can produce new plants and thereby help in the conservation of *P. kurroa*. In previous studies, various

strategies have been employed to enhance P-I content in *P. kurroa* shoots including; optimization of media compositions and use of various elicitors, but P-I content in tissue cultured grown *P. kurroa* shoots was ~4-5 times lesser compared to plants grown in natural habitat [21-22]. To address this problem, metabolic engineering is the only alternative to maximize the production of P-I and P-II in shoot cultures by redirecting the carbon flux towards picrosides biosynthesis. However, it requires prior knowledge of biosynthetic pathways and associated key steps regulating P-I and P-II production.

The biosynthetic pathways for P-I and P-II were proposed including; non-mevalonate (MEP), mevalonate (MVA), shikimate/phenylpropanoid (S/P) and iridoid pathways [23]. In addition, numerous efforts have also been carried out to shortlist candidate genes involved in P-I and P-II biosynthesis through gene expression analyses vis-à-vis picrosides accumulation in *P. kurroa* [24-25]. Despite interesting cues obtained from these reports, yet this remains a formidable task considering the fact that biosynthetic architecture of picrosides is complex, non-linear and fluxes dynamics is poorly understood. Till date, no information is available on what mechanism controls the flux of P-I and P-II biosynthesis in *P. kurroa* and which out of the different modules are limiting for their supply? Further, why P-II is not produced in *P. kurroa* shoots? It is, therefore, crucial to understand the mechanism behind P-I and P-II biosynthesis in *P. kurroa* prior to designing a suitable metabolic engineering approach.

It has been widely known that secondary metabolic pathways are dependent on primary metabolism for the supply of precursors. Therefore, proper execution of P-I and P-II biosynthesis requires the coordination of a more number of primary and secondary pathways which further pose a challenge to shortlist these numerous enzymes in order to select the suitable targets for their enhanced production in *P. kurroa.* To elucidate the metabolic flux dynamics, radioactive/stable isotopes labelled flux analysis have been executed in various plant species but concurrently accompanied with cost intensive and time consuming experiments. Thus, we address this issue here with feeding of different precursors in the context of picrosides biosynthesis in *P. kurroa*. It has been reported that exogenous feeding of precursors situated at the key biosynthetic steps can stimulate the production of target secondary metabolites in *in vitro* conditions, provided the endogenous levels of selected precursors are a limiting factor for the target metabolite biosynthesis [26]. Several reports have shown the influence of precursor availability on the accumulation of target metabolites and metabolic flux limitations. For example, exogenous tryptamine and loganin have been reported to increase the levels of secologanin in transgenic cell lines of *Catharanthus roseus* and utilization of supplied precursors determined the metabolic flux through the pathway components [27]. Despite the potential of precursor's feeding in the elucidation of metabolic routes of P-I production, yet this is not applicable for P-II biosynthesis as P-II has not been produced under *in vitro* conditions. Therefore, it is a challenge to resolve the complexity of P-II biosynthesis as both protocatechuate and ferulic acid; the metabolites of S/P pathway, are plausible to produce vanillic acid, the immediate precursor of P-II [23, 28]. The mature stolons were proposed to be the independent biosynthetic organs as evident by the analysis of P-I and P-II contents in different developmental stages of *P. kurroa* [1]. Therefore, we have selected mature stolons to elucidate the mechanism controlling P-II biosynthesis in *P. kurroa*. We have utilized natural variations in P-II content among different accessions of *P. kurroa* so as to guide us in discerning the route and flux of intermediates leading to the P-II biosynthesis. Moreover, the integration of metabolites contents data with the corresponding

transcriptomes would enable us to understand the flux of intermediates vis-à-vis gene transcripts controlling P-II biosynthesis in *P. kurroa*.

Therefore, in light of the immense need to elucidate contributions of different modules in picrosides biosynthesis to enable their rational metabolic engineering in *P. kurroa*, the present research work was designed with the following objectives:

Objectives

1. Elucidation of connecting links between primary and secondary metabolism in the context of picrosides biosynthesis in *P. kurroa*
2. Elucidation of key steps contributing to P-I biosynthesis through intermediates flux dynamics in *P. kurroa*
3. Elucidation of metabolic route and associated key steps for P-II biosynthesis in *P. kurroa*

Materials and methods

Collection of plant material

Field grown plants along with 10 accessions of *P. kurroa* were collected from nursery (Jagatsukh, H.P.) and kept in the greenhouse of Jaypee University of Information Technology, Waknaghat, H.P., India. The plants were segregated into shoots, mature stolons and roots, which were labelled as PKS, PKST and PKR, respectively. The field grown plants of *P. kurroa* were then cultured in an optimized Murashige and Skoog (MS) medium supplemented with 3 mg/L indole-3-butyric acid (IBA) and 1 mg/L kinetin (KN) and incubated in a plant tissue culture chamber maintained at 25±1°C. After 6 weeks, the *P. kurroa* shoots were taken as an explant for carrying out further experimentation at 15°C where *in vitro* grown shoots were incubated and the shoot samples were collected at 0, 10, 20, 30 and 40 days after the start of the experiment. All the samples were kept at -80°C for further analyses.

Precursors feeding experiments

Addition of different precursors for P-I

The solutions of different precursors; cinnamic acid (CA) at 70, 150 and 230 µM concentrations while catalpol (CAT) at 30, 70 and 150 µM concentrations, were prepared alone as neutral aqueous stocks. In contrast, different combinations of CA+CAT mixture viz. 70 µM CA+30 µM CAT, 150 µM CA+70 µM CAT and 230 µM CA+150 µM CAT, were also prepared as neutral aqueous stocks and tested for their effects on P-I production. These solutions were filter sterilized directly into culture flasks containing optimized MS medium supplemented with 3 mg/L IBA and 1 mg/L KN. Shoot cultures of *P. kurroa* grown at 25°C were aseptically transferred to these culture flasks and kept at 15°C in a plant tissue culture chamber. Shoots of *P. kurroa* grown at 15°C without any treatment were used as controls. After 30 days, the cultures were harvested and shoot samples were immediately stored at −80°C for further analyses.

Addition of different precursors for P-II

The solutions of different precursors; p-coumaric acid (p-CA), protocatechuate (PA) and ferulic acid (FA) were prepared as neutral aqueous stocks at 150 µM concentrations. Conversely, different concentrations of VA+CAT mixture viz. 25 µM each VA+CAT, 70 µM each VA+CAT, 70 µM VA+150 µM CAT, 150 µM VA+70 µM CAT, 150 µM each

VA+CAT and 230 µM each VA+CAT, were used for the feeding of *in vitro* grown *P. kurroa* shoots. Moreover, 25 µM P-II was also introduced separately in the MS medium to check the accumulation of P-II in *P. kurroa* shoots. In addition to this, the solutions of VA+CAT mixture (70 µM) and P-II (25 µM), were also checked for the intake of precursors by the plant in liquid cultures. Following this, the culturing of *P. kurroa* shoots was performed according to the same protocol as mentioned above. The shoots without precursor treatment were labelled as controls. The shoot samples were harvested after 30 days and immediately stored at -80°C for further analyses.

Extraction and quantification of picrosides

Each powdered sample (100 mg) was homogenized in a prechilled mortar and pestle using liquid nitrogen and suspended in 10 mL of 80% methanol, vortexed followed by sonication at room temperature (RT) for 30 min and centrifuged at 10,000 rpm for 15 min. The supernatants were filtered through 0.22 µm filter, diluted 10-fold with 80% methanol and used for quantification of P-I and P-II by HPLC. In HPLC, C18 reverse phase column (4.6×250 mm, 5 µm) was used for the separation of compounds. The mobile phase was made up of distilled H_2O:methanol:acetonitrile in a ratio of 70:15:15 (containing 0.03% trifluoroacetic acid). The column was eluted in the isocratic mode with flow rate of 1.0 mL/min and the cycle time of analysis was 30 min at 30°C. The picrosides were detected at a wavelength of 280 nm and identified on the basis of their retention time and comparison with UV spectra of standards (ChromaDex).

Extraction and quantification of intermediate metabolites

The samples (200mg) in triplicates were homogenized with liquid N_2 in prechilled pestle and mortar; suspended in 7 mL of combination of methanol (containing 2g/L butylated hydroxytoluene) and 10% acetic acid in a ratio of 85:15 and vortexed for 10 min at RT. The volume of extracts was made up to 10 mL with distilled H_2O. To each extract, 12 mL of distilled H_2O and 5 mL 10M sodium hydroxide were added and bubbled with N_2 gas, sealed and kept on a magnetic stirrer for overnight at RT. Next day, the pH of extracts was adjusted to 2 and metabolites were extracted three times with 15 mL of a mixture of cold diethyl ether and ethyl acetate in a ratio of 1:1 by shaking and centrifuging. The diethyl ether/ethyl acetate layers were evaporated to dryness and reconstituted in 1.5 mL of 100% methanol. The samples were filtered through 0.22 µm filter and subjected to quantification of selected metabolites in triplicates by using HPLC as per the method described in Nour et al. [29]. The selected compounds viz. CA, p-CA, FA, PA and VA were detected at a wavelength of 290±4, 310±4, 330±4, 260±4 and 260±4 nm, respectively. All the selected compounds were identified upon comparison of retention time and UV spectra with standards.

RNA isolation, cDNA synthesis and gene expression analysis

Total RNA was isolated by using TRIzol reagent (Ambion) as per the manufacturer's instructions. The quantification of isolated RNA was carried out at 260/280 nm wavelengths with ND-2000 UV spectrophotometer and quality was checked on 1% agarose gel stained with ethidium bromide. Synthesis of cDNA was performed from 5 µg of total RNA using Verso cDNA synthesis kit as per the manufacturer's instructions. The resulting cDNA was quantified to obtain equal concentration (100 ng) by using ND-2000 UV spectrophotometer. The primers of the selected genes were designed from transcriptomic sequences of *P. kurroa* by using Primer3 software. The gene expression analysis was conducted in triplicates on

CFX96 system (Bio-Rad) with the standard 96 well block. The reaction mixture (12.5 µL) used for qPCR analysis contained: 0.5 µL forward primer (10 pmol), 0.5 µL reverse primer (10 pmol), 6.25 µL iQTM SYBR Green Supermix (BIO-RAD), 1 µL cDNA (100 ng) and 4.25 µL nuclease free H_2O. The qPCR programme was: (1) 1 cycle of 95°C for 3 min; (2) 39 cycles of 95°C for 10 s, 49–60°C for 20 s and 72°C for 20 s followed by a final melt curve analysis. The 26S was used as the reference gene.

Extraction and determination of enzymes activities

Each sample was homogenized in a prechilled mortar and pestle using liquid N_2 with 5 mL of extraction buffer, which varied in composition for different enzymes: hexokinase (HK) and malate dehydrogenase (MDH) [0.1M Tris-Cl pH 7.5 containing 50mM β-mercaptoethanol (β-ME), 5mM $MgCl_2$, 50mM sucrose, 1% Triton X-100 and 1% insoluble PVP (w/v)]; pyruvate kinase (PK) [50mM Tris-Cl pH 7.5 containing 10mM $MgSO_4$, 5mM β-ME, 20% ethylene glycol (v/v) and 1% insoluble PVP (w/v)]; isocitrate dehydrogenase (ICDH) [50mM Na-phosphate pH 7.5 containing 5mM $MgCl_2$ and 1% insoluble PVP (w/v)], $NADP^+$- malic enzyme (ME) [0.1M Tris-Cl pH 7.5 containing 5mM $MgCl_2$, 10mM β-ME, 10% glycerol (v/v), 1mM PMSF and 1% insoluble PVP (w/v)], and phenylalanine ammonia lyase (PAL) [100 mM sodium borate buffer, pH 8.8, containing 5 mM β-ME]. The homogenate was then centrifuged at 10,000xg for 30 min and the supernatant was dialyzed overnight against ten times diluted extraction buffer lacking PVP. The overnight dialyzed extract was centrifuged at 10,000xg for 20 min and the supernatant was used for enzyme assays.

The standard assay mixture for PAL contained 100 mM Na borate buffer (pH 8.8), 15 mM phenylalanine (Phe) and 50 µL crude extract in a total volume of 3.0 mL. The mixture without Phe was preincubated at 30°C for 20 min to allow for an initial non-enzymatic decrease in absorbance and then the reaction was initiated by the addition of Phe. The increase in absorbance was recorded over a period of 60 min at 290 nm wavelength using a UV-VIS spectrophotometer. The PAL activity was determined by standard curve prepared by taking different concentrations of CA. The activity of PAL was expressed as µmol of CA formed/min/mL under the specified conditions and data has been reported as milliunits (mU) of enzyme. The activities of rest of the enzymes in crude extracts were determined using coupled assays. The absorbance was recorded using a UV-VIS spectrophotometer. The standard assay mixture for HK contained 50mM Tris-Cl buffer pH 7.5, 5mM $MgCl_2$, 1mM $NADP^+$, 5mM glucose, 2.5mM ATP, G-6-P dehydrogenase (2.25 U) and 200 µL crude extract in a total volume of 3.0 mL. The reaction carried out at 30°C was initiated by the addition of ATP. The enzyme activity has been expressed as µmol $NADP^+$ reduced min^{-1} at 340 nm under the specified conditions. The standard assay mixture for PK contained 50mM Tris-Cl buffer pH 7.2, 10mM $MgSO_4$, 50mM KCl, 0.1mM NADH, 1.8mM ADP, 1.2mM PEP, LDH (2 U) and 50 µL crude extract in a total volume of 1.0 mL. The reaction carried out at 30°C was initiated by the addition of PEP. The enzyme activity has been expressed as µmol NADH oxidized min^{-1} at 340 nm under the specified conditions. The assay mixture for ICDH contained 50mM Tris-Cl buffer pH 7.5, 5mM $MgCl_2$, 1mM $NADP^+$, 10mM DL-isocitrate and 100 µL crude extract in a total volume of 3.0 mL. The reaction carried out at 30°C was initiated by the addition of DL-isocitrate. The enzyme activity has been expressed as µmol $NADP^+$ reduced min^{-1} at 340 nm under the specified conditions. The activity of MDH was assayed in a reaction mixture containing 50mM potassium phosphate buffer pH 7.0, 0.15mM NADH, 1mM oxaloacetate and 100 µL crude extract in a total volume of 3.0

mL. The reaction carried out at 30°C was initiated by the addition of oxaloacetate. The enzyme activity has been expressed as µmol NADH oxidized min^{-1} at 340 nm under the specified conditions. The assay mixture for $NADP^+$-ME contained 50mM Tris-Cl buffer pH 7.5, 10mM $MgCl_2$, 0.5mM NADP, 10mM L-malate and 100 µL crude extract in a total volume of 3.0 mL. The reaction carried out at 30°C was initiated by the addition of L-malate. The enzyme activity has been expressed as µmol $NADP^+$ reduced min^{-1} at 340 nm under the specified conditions. The Protein content in all extracts was estimated by Lowry's method.

Preparation of libraries, sequencing, transcriptome *de novo* assembly and validation

The construction of libraries and their sequencing for transcriptome analysis was performed as per the protocol described in Pal et al. [30]. For *de novo* assembly, we chose gowith De brijn graph based Trinity Assembler based on the criteria of; a) default K-mer, b) less memory foot print, c) optimized for Illumina paired end data, d) reproducibility and, e) configurable for all computing capacities. To pool assembly, 50 core threads of processing with 2.4 GHz speed and a maximum Heap Space of 50 GB was allotted. Nevertheless, *de novo* transcriptome assemblers are capable of producing in fragmented/miss-assembly, the validation of assembled transcriptome was carried out by mapping back the high quality (HQ) filtered reads to the ESTs. The HQ filtered reads from each library thus obtained were mapped to the assembled transcriptome by using Bowtie software. This analysis generated .bam (Binary Sequence Alignment/Map) files which were processed through bedtools and samtools for quantitation (read count estimation) of each transcript in a library and also to calculate the total coverage and average depth of the transcriptome in each library [31-32].

Transcripts annotation

The annotation and statistical analysis of each transcript was performed by homology based method against NCBI nrdb protein database using Blast2GO software through Blastx module. The parameters used for this analysis were; a) e-Value b=10−e4, b) Similarity ≥ 35%, c) Annotation cutoff ≥ 55, d) GO weight cutoff ≥ 5. Moreover, domain level annotation was also performed by using the Online InterProScan tool RunIprScan-1.1.0 (http://michaelrthon.com/runiprscan/).

Normalization of transcripts and their expression profiling

Transcripts with a read count of ≥10 in any one of the libraries were considered to be expressed. To perform normalization and expression profiling, a sub bam file was created from the master bam file using RSEM software. In RSEM, the default parameters/commands were used to normalize each library which provides an output with expected normalized read count, TPM (Tags Per Million) and FPKM (Fragments Per Kilobase Per Million). Log to the base 2 of FPKM was considered as absolute expression or ΔCt equivalent value.

Transcripts mapping, DEG and correlation analysis

The annotated transcripts obtained from BLAST2GO were mapped to Kyoto Encyclopedia of Genes and Genomes (KEGG). Transcripts which were involved in secondary metabolic pathways were shortlisted for differentially expressed gene (DEG) analysis using sequence similarity threshold of >98%. Only those transcripts were selected and used for the analyses which were present in all the 8 different samples i.e. 4 accessions of each shoots and stolons. Hierarchical clustering of selected DEGs were performed using heatmaply, gplot2, plotly packages in R. Further, the correlation analysis was carried out by using R-package through "Corrgram" function.

Statistical analysis

The statistical analysis was performed from mean±SD of data in triplicates by using one and two-way analysis of variance (ANOVA) followed by a Bonferroni test using GraphPad prism software version 6.0.

Results

Picrosides (P-I and P-II) contents in different growth conditions of *P. kurroa*

The field grown *P. kurroa* shoots contained 1.4% P-I, which was 2.8-fold greater in shoots grown under tissue cultures at 15°C (0.5%) while P-I was not detected in the shoots grown at 25°C. In addition, *P. kurroa* shoots also showed significant variations in P-I content at 0, 10, 20, 30 and 40 days of plant growth. The P-I content increased from 0 to 0.19 µg/mg from 0 to 10 days, followed by 2.16-fold increase at 20 days compared to 10 days stage. At 30 days, the P-I content showed 4.07-fold increase over 20 days but remained constant at 40 days stage.

The analysis of shoot tissues of *P. kurroa* accessions revealed maximum P-I content in PKS-1 which showed 1.9-, 2.1-, 2.3-, 2.5-, 3.4-, 3.6-, 3.6-, 4.7- and 17.7-fold increment over PKS-5, PKS-2, PKS-3, PKS-26, PKS-16, PKS-18, PKS-14, PKS-4 and PKS-21, respectively (Fig. 1a). In contrast, P-II was not detected in shoots of *P. kurroa* plants. These results implies that PKS-1 and PKS-5 showed maximum P-I content, while PKS-4 and PKS-21 contained minimum P-I content and thus, referred to as high and low P-I content accessions of *P. kurroa*, respectively. Conversely, stolons tissues of *P. kurroa* accessions showed maximum P-II content in PKST-3 (2.65%) and then progressively decreased leading to PKST-18 with 1.9-fold lower P-II content (Fig. 1b). Further, minimum P-I content (0.08%) was detected in PKST-5 followed by 2-fold non-significant increase in PKST-3 stolon. The stolons of PKST-1, PKST-2, PKST-14, PKST-26, PKST-16 and PKST-18 showed progressive increase in P-I content with 5.3-, 8.6-, 8.8-, 10.2-, 13.1- and 16.5-fold, respectively compared to PKST-5 (Fig. 1b). Thus, PKST-3 and PKST-5 stolons were referred to as high P-II content accessions, while PKST-16 and PKST-18 as low P-II content accessions of *P. kurroa*.

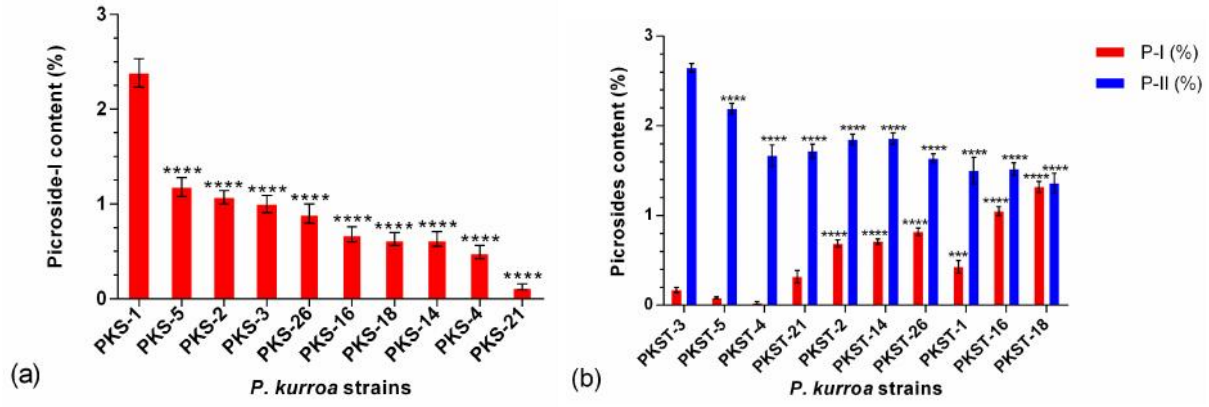

Fig. 1. Determination of picrosides contents in different tissues of *P. kurroa* accessions; (a) shoots and, (b) stolons. The data showed means±SD (n=3). Significance was evaluated within picrosides contents between different accessions. (***p<0.001, ****p<0.0001)

Alterations of intermediate metabolites among selected *P. kurroa* accessions

The analyses of shoot tissues revealed maximum CA content (0.5%) in PKS-1 which showed progressive decrease in PKS-5, PKS-4 and PKS-21 with 1.5-, 2.5- and 5.3-fold, respectively. In contrast, the lowest p-CA content (0.04%) was observed in PKS-1 and showed increase in

PKS-5 and PKS-21 with 2.1- and 5.9-fold, respectively (Fig. 2e). The FA content in shoot tissues showed 2-fold elevation in PKS-21 compared to PKS-1, PKS-5 and PKS-4 accessions; while VA content showed no alterations in all the four shoots of *P. kurroa*. The PA content was not detected in the *P. kurroa* shoots. These results imply positive correlation of CA with P-I content in shoots with Pearson correlation coefficient (PCC) of 0.99 (Fig. 2f).

The investigation of stolons revealed maximum CA content (0.2%) in PKST-18 which showed 4.7-fold increase over PKST-3; while p-CA content showed no alterations in the four stolons of *P. kurroa* (Fig. 2b). The FA content showed highest level in PKST-5 (0.2%) which exhibited 1.7-fold increase over PKST-3, PKST-16 and PKST-18. Further, VA content was maximum in PKST-3 and PKST-5 followed by decrease in PKST-16 and PKST-18 with 2.2- and 1.3-fold, respectively. However, PA content was not detected in the stolons of *P. kurroa*. These observations infer positive correlations of p-CA and VA with P-II through PCC of 0.45 and 0.79, respectively (Fig. 2c).

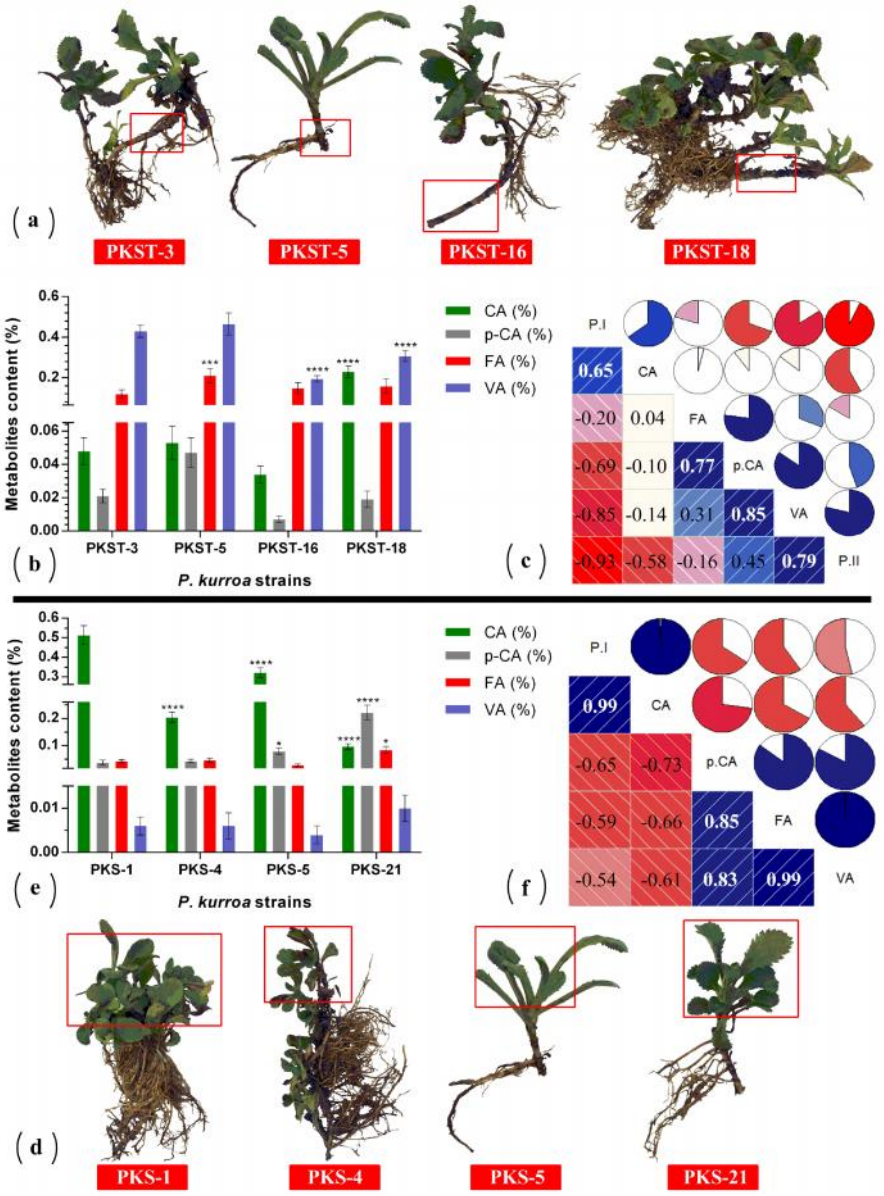

Fig. 2. Intermediate metabolites contents among different tissues of *P. kurroa* accessions; (a, d) *P. kurroa* accessions for stolons and shoots, respectively; (b, e) variations in metabolites contents between stolons and shoots, respectively and; (c, f) correlogram showing

correlations between tested metabolites and picrosides contents among stolons and shoots, respectively. Correlations are presented in the form of pie graphs filled in proportion to the PCC values. Clock-wise filled with blue color depict positive correlations while anti-clockwise filled with red color indicate negative correlations. The data showed means±SD (n=3). Significance was evaluated within metabolites contents between different accessions. (*p<0.05, ***p<0.001, ****p<0.0001).

Effect of different precursors on contents of intermediate metabolites and picrosides

Among the tested concentrations of CA and CA+CAT, increment in P-I content was observed with 1.6- and 4.2-fold, respectively at 150 µM CA and 150 µM CA+70 µM CAT concentrations compared to untreated control shoots. In contrast, the CAT alone showed non-significant increase in P-I content compared to control. These observations infer 150 µM CA and 150 µM CA+70 µM CAT as optimum concentrations for further precursor's treatments. Moreover, the analysis of *P. kurroa* shoots treated with optimum concentrations of CA, CAT and CA+CAT for p-CA and CA contents, revealed 1.5-fold increased p-CA content in shoots treated with CA while non-significant increase was observed in CAT and CA+CAT treated shoots compared to control (Fig. 3a). In contrast, CA content showed 3.8-fold increase in CA+CAT treated shoots while no effect was observed in CA and CAT treated shoots compared to control (Fig. 3b).

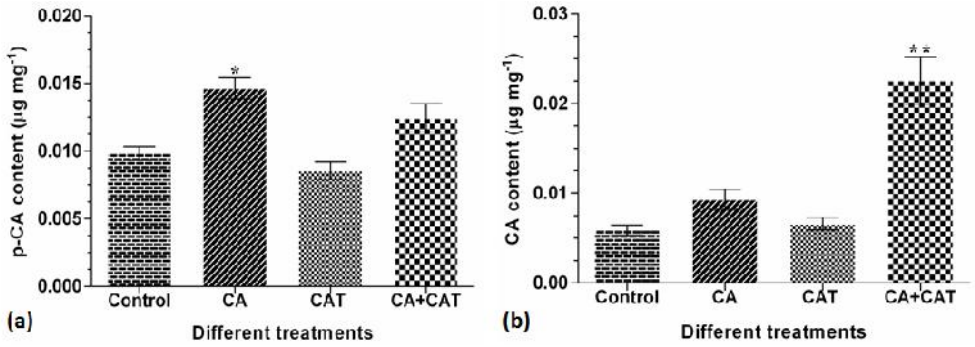

Fig. 3. Influence of different precursor treatments on the production of; (a) p-CA, (b) CA. The data showed means±SD (n=3). Significance was evaluated between different treatments and untreated control. (*p<0.05, **p<0.01).

Further, the *in vitro* grown *P. kurroa* shoots treated with 150µM concentration of PA, FA and p-CA along with combination of 150µM VA and 70µM CAT, revealed 2.2- and 1.7-fold increase of CA content in shoots treated with FA and p-CA, respectively, whereas 1.3-fold decrease was observed in VA+CAT fed shoots compared to control (Fig. 4a). The p-CA content was not modulated in all the fed shoots compared to control. The analysis of FA content revealed 2.9-fold increase FA treated shoots over control. In contrast, 1.9- and 2-fold increased VA content was observed in shoots fed with FA and VA+CAT, respectively compared to control (Fig. 4a). Moreover, the P-I content showed 1.8-fold enhancement in p-CA fed shoots compared to control. Interestingly, small level of P-II i.e. 0.04% was only detected in *P. kurroa* shoots treated with VA+CAT (Fig. 4a). These results infer high positive correlation between VA and P-II with PCC of 0.64 and the former was also positively correlated with CA and FA with PCC of 0.19 and 0.22, respectively (Fig. 4c). Since, P-II was only detected in VA+CAT fed shoots therefore, different concentrations of VA+CAT were further tested but showed non-significant alterations in P-II content (Fig. 4b). Moreover, the

P-II content also exhibited non-significant alteration in shoots fed with P-II while 0.2% P-II was observed in the media remained after the sampling of shoots treated with P-II (Fig. 4b).

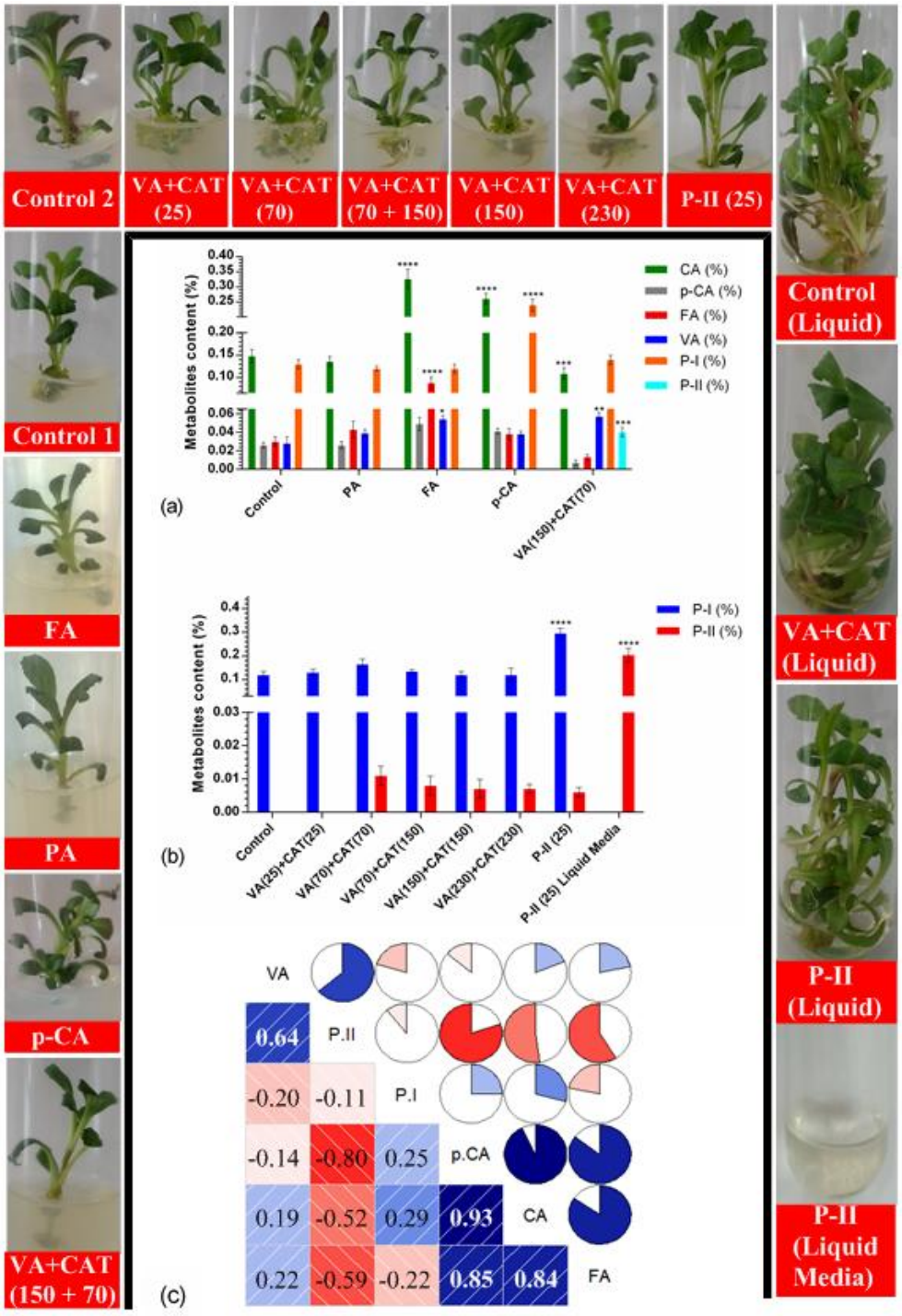

Fig. 4. Alterations in the levels of tested metabolites among different fed samples; (a) PA, FA and p-CA at 150 µM concentration along with 150 µM VA + 70 µM CAT; (b) variations in picrosides contents among different concentrations of VA+CAT along with P-II and liquid media remained after the collection of samples and; (c) correlogram showing correlations between tested metabolites and picrosides contents among different precursors treated samples. The data showed means±SD (n=3). Significance was evaluated within metabolites contents between different precursor's treatments. (*p<0.05, **p<0.01, ***p<0.001, ****p<0.0001)

Gene expression profiles vis-a-vis picrosides biosynthesis in differential conditions

The transcript level of HK in field grown shoots was 8- and 87-fold greater compared to plants grown at 15°C and 25°C, respectively. Similarly, transcript level of PK in field grown shoots was 12.6- and 81.2-fold greater than shoots grown at 15°C and 25°C, respectively. For the TCA cycle enzymes, the expression of ICDH gene was 18- and 54.3-fold higher whereas that of MDH gene was 1.7- and 13.9-fold superior in 15°C shoots as compared to *P. kurroa* shoots grown in field and at 25°C, respectively. The transcript level of $NADP^+$-ME in 15°C grown shoots was 1.7-times greater than in field grown shoots but 23.6-fold greater than in plants grown at 25°C (Fig. 5). These observations infer that the selected enzymes of primary metabolism might be involved in P-I biosynthesis.

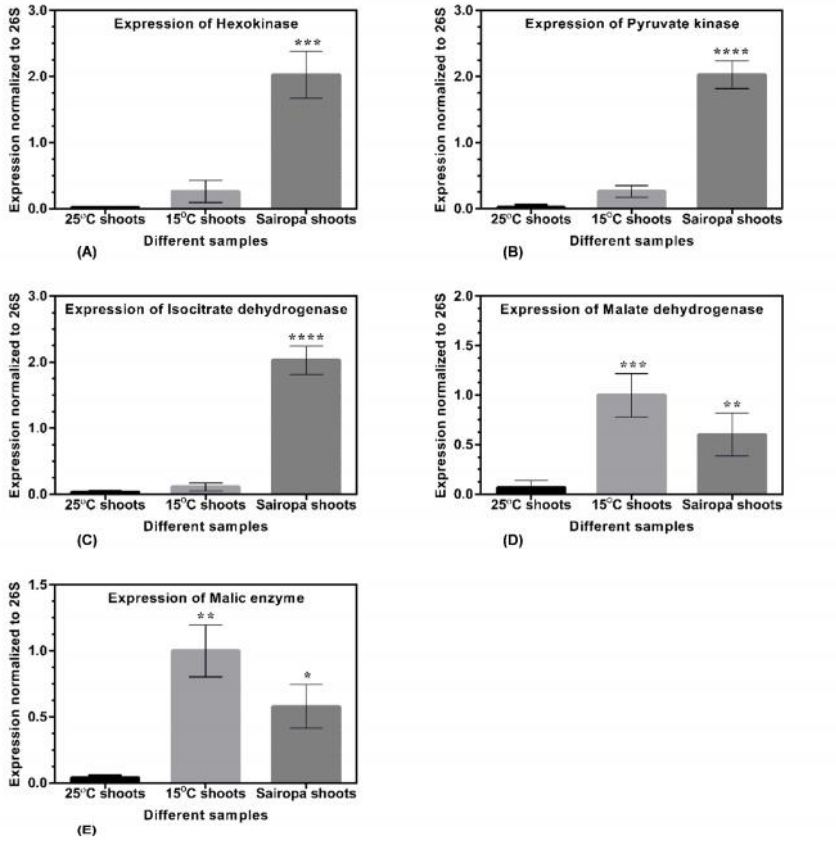

Fig. 5. Gene expression profiles of glycolysis (HK, PK), TCA cycle (ICDH, MDH) and NADP+-ME enzymes' in *P. kurroa* shoots grown in field and in tissue culture conditions (15°C and 25°C). Expression levels were normalized to housekeeping gene *i.e.* 26S. The data showed means ± SD (n = 3). Significance was evaluated between 15°C, field grown and 25°C condition (*p<0.05, **p<0.01, ***p<0.001, ****p<0.0001).

Expression profiling of selected genes in different growth stages of P. kurroa

The expression profiles of 13 genes belonging to glycolysis (HK and PK), TCA cycle (ICDH and MDH), pentose phosphate pathway (G-6-PDH), MVA pathway (HMGR and PMK), MEP pathway (DXPS and ISPD), S/P pathway (DAHPS and PAL) and iridoid pathway (GS and G-10-H) were observed at 0, 10, 20, 30 and 40 days of *P. kurroa* growth at 15°C. The results revealed that expression of all the above selected genes at 10 days appeared to be similar to 0 day stage. However, in 20 days grown shoots, the expression of HK, PAL and G-10-H genes showed <20-fold increase over the 10 days stage while the expression of G-6-PDH, MDH, DXPS, HMGR, PMK and GS genes augmented between 20- to 30-folds (Fig.

6). In contrast, the transcript levels of DAHPS, ISPD, PK and ICDH showed an increase of 44-, 77-, 81.5- and 130-fold, respectively. Upon analysis of 30 days grown shoots, down- and up-regulation of 5 and 8 genes, respectively were observed compared to 20 days stage (Fig. 6). The HK, DXPS, ISPD, HMGR and PMK genes were down-regulated by 0.30-, 0.32-, 0.01-, 0.38-, and 0.05-fold, respectively whereas the expression of DAHPS, PAL, G-6-PDH, PK, ICDH, MDH and GS genes was up-regulated by 4.56-, 1.97-, 1.81-, 1.61-, 1.40-, 2.64- and 1.42-fold, respectively. Further, G-10-H gene exhibited most up-regulated expression with 6.15-fold at 30 days stage compared to 20 days (Fig. 6). At 40 days stage, a striking decrease in the transcript level of HK, DXPS, HMGR, DAHPS, PAL, G-6-PDH, PK, ICDH, MDH, GS and G-10-H was observed to the tune of 0.49-, 0.73-, 0.52-, 0.01-, 0.02-, 0.02-, 0.02-, 0.13-, 0.01-, 0.04- and 0.05-fold, respectively. On the other hand, the expression of ISPD and PMK genes was up-regulated by 26.5- and 1.24-fold, respectively as compared to 30 days of growth but down-regulated by 0.14- and 0.06-fold, respectively in comparison to 20 days stage, indicating their involvement in the regulation of P-I biosynthesis (Fig. 6).

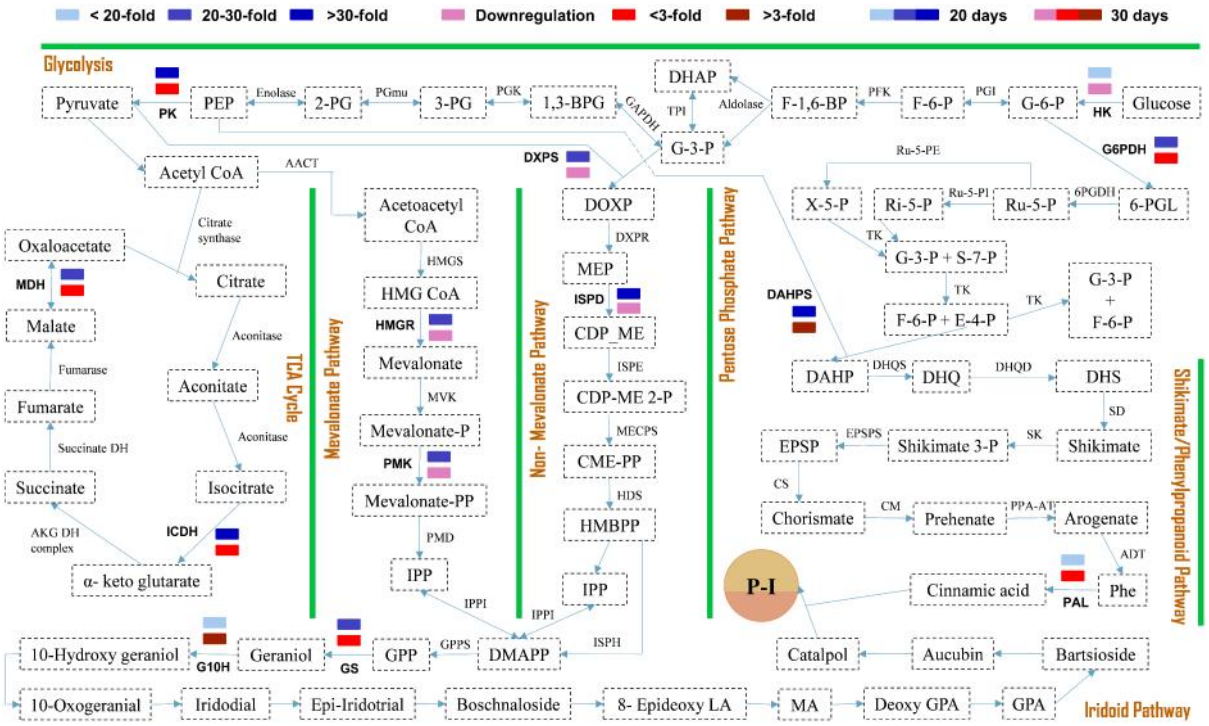

Fig. 6. An outline of the primary and secondary metabolism which integrates into P-I biosynthesis. The metabolic network has been reconstructed by including glycolysis, TCA cycle, pentose phosphate pathway, S/P, MVA/MEP and iridoid pathway. Squares coded with different colors highlighted the expression of genes encoding enzymes examined in the primary and secondary metabolism at different time intervals of *P. kurroa* growth; after 20 days (blue color) and, after 30 days (red color).

Expression status of selected genes in shoots treated with different precursors

Among the shoots treated with CA+CAT, DAHPS and CM were up-regulated by 2.4- and 1.8-fold, respectively whereas PAL, C4H and GS were down-regulated by 6.2-, 1.4- and 2.4-fold, respectively, compared to control. In contrast, the transcript encoding G10H showed no alteration compared to untreated control shoots. However, shoots treated with CA showed down-regulation of CM and PAL transcripts with 3- and 8.2-fold, respectively whereas transcripts encoding DAHPS, C4H, GS and G10H enzymes showed non-significant

modulation compared to control. Further, the CAT treated shoots revealed down-regulation of C4H, GS and G10H transcripts with 1.5-, 12.9- and 2.7-fold, respectively whereas transcripts encoding DAHPS, CM and PAL enzymes showed non-significant modulation compared to control shoots (Fig. 7).

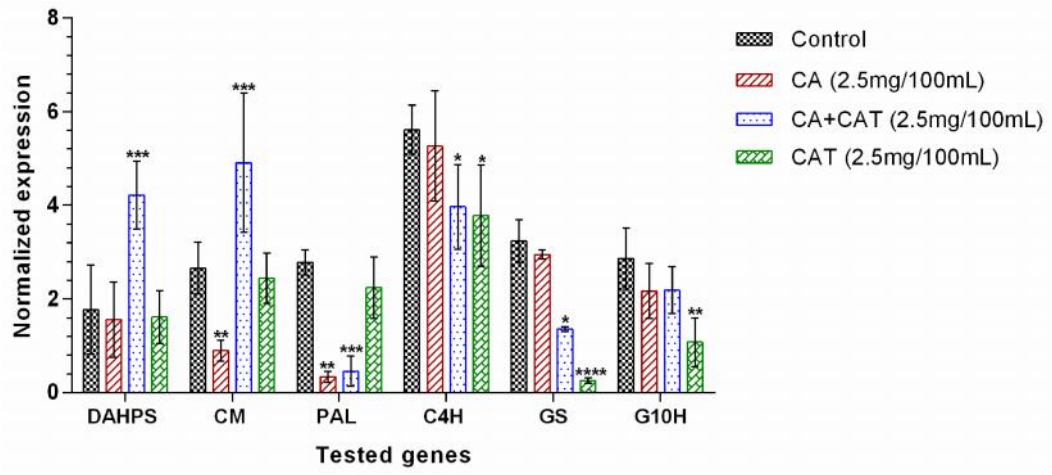

Fig. 7. Expression profiles of selected shikimate/phenylpropanoid and iridoid pathways genes in CA, CAT and CA+CAT fed shoot cultures of *P. kurroa*. Expression levels were normalized to 26S reference gene expressions. The data showed means±SD (n=3). Significance was evaluated for each gene between different treatments and untreated control (**p*<0.05, ***p*<0.01, ****p*<0.001, *****p*<0.0001).

Activity profiles of selected enzymes in differential conditions of picrosides biosynthesis

For glycolytic enzymes, specific activity of HK was 0.032, 0.0176 and 0.004 µmoles $NADP^+$ reduced min^{-1} mg^{-1} protein whereas that of PK was 0.268, 0.055 and 0.043 µmoles of NADH oxidized min^{-1} mg^{-1} protein in the field grown shoots, at 15°C and 25°C, respectively (Fig. 8). The activity profiles of TCA cycle enzymes showed that in field grown shoots, specific activity of ICDH was 11.7-fold and 35.7-fold higher whereas that of MDH was 1.2-fold and 4.0-fold greater than in shoots at 15°C and at 25°C, respectively. The pattern of $NADP^+$-ME activity was somewhat different; its activity was maximum in shoots at 15°C followed by field grown shoots and lowest in shoots grown at 25°C (Fig. 8). These results revealed a positive correlation between the specific activity of selected enzymes and the P-I content in different conditions of plant growth, indicating the importance of these primary metabolic pathway enzymes in the accumulation of P-I.

The analysis of CA, CAT and CA+CAT fed shoots of *P. kurroa* revealed significant variations in the activity of PAL enzyme compared to untreated control shoots. The PAL activity was down-regulated by 1.2-fold in shoots fed with CA while up-regulated by 1.2-fold in CA+CAT fed shoots compared to untreated control. In contrast, the activity of PAL enzyme showed non-significant alteration in CAT treated shoots compared to control shoots (Fig. 9).

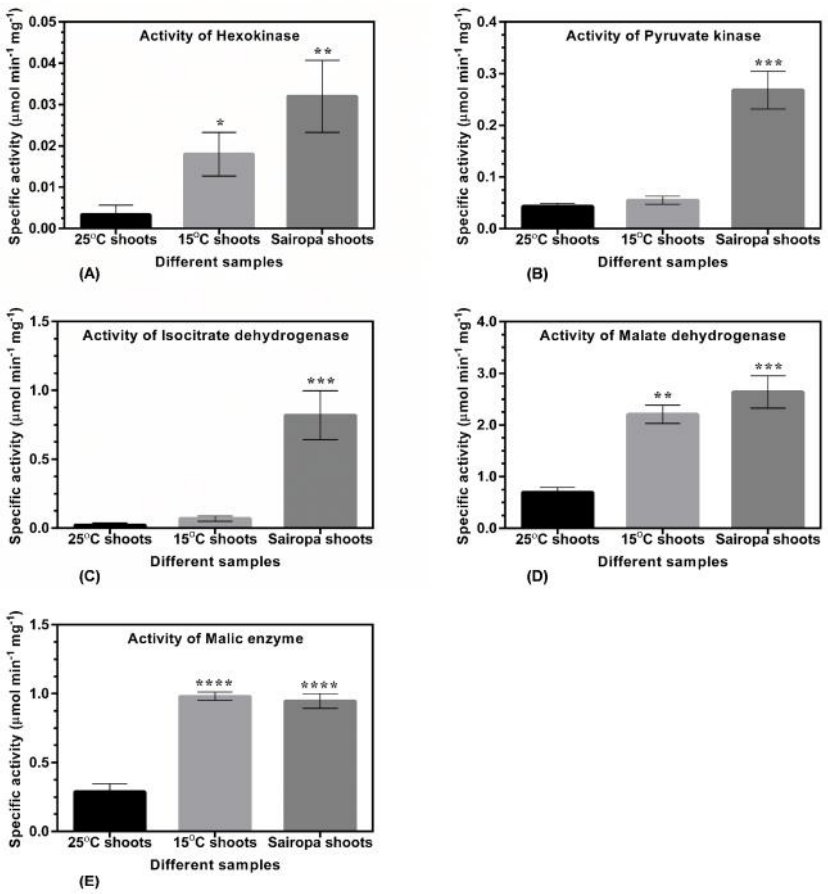

Fig. 8. Catalytic activities of glycolysis (HK, PK), TCA cycle (ICDH, MDH) and NADP+-ME enzymes' in *P. kurroa* shoots grown in field and in tissue culture conditions (15°C and 25°C). The data showed means ± SD (n = 3). Significance was evaluated between 15°C, field grown and 25°C condition (*p<0.05, **p<0.01, ***p<0.001, ****p<0.0001).

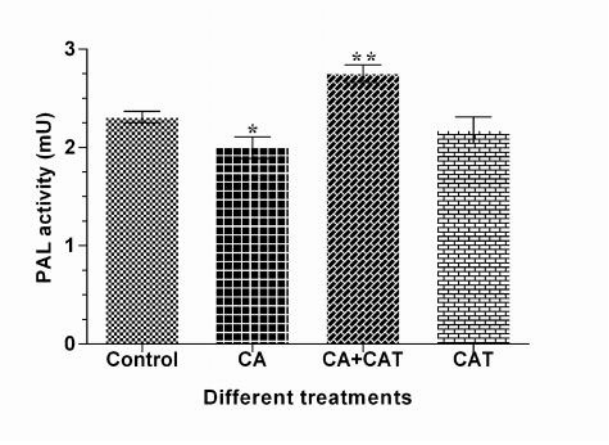

Fig. 9. Activity profiles of PAL in CA, CAT and CA+CAT fed shoot cultures of *P. kurroa*. The data showed means ± SD (n = 3). Significance was evaluated between different treatments and untreated control (*p<0.05, **p<0.01).

Correlation analysis

The significant positive correlations (PCC, r>0.79) were observed between enzyme activity and gene expression among all the selected five enzymes (HK, PK, ICDH, MDH and $NADP^+$-ME) in field grown as well as tissue culture grown (15°C and 25°C) shoots of *P.*

kurroa. The PCC of ICDH (r=0.9994) was observed as the highest followed by PK (r=0.9977), $NADP^+$-ME (r=0.9161) and HK (r=0.8837); whereas MDH (r=0.7925) showed minimum correlation coefficient. These significant positive correlations under differential conditions of picroside biosynthesis indicated the involvement of these enzymes in P-I accumulation.

Moreover, the correlations were also observed among selected genes and tested metabolites (P-I, CA and p-CA) levels between different precursors treatments (control, CA, CAT and CA+CAT). The analysis revealed positive correlation of P-I with CA (0.99), DAHPS (0.97) and CM (0.78) while low correlation was observed with p-CA (0.31) and G10H (0.14) (Fig. 10). In contrast, negative correlations of P-I were observed with PAL, GS and C4H genes. We have thus been able to assess from the correlations that DAHPS, CM, CA and G10H might play a crucial role in the biosynthesis of P-I whereas PAL and GS could be the potential regulatory sites of P-I biosynthesis in shoot cultures of *P. kurroa*.

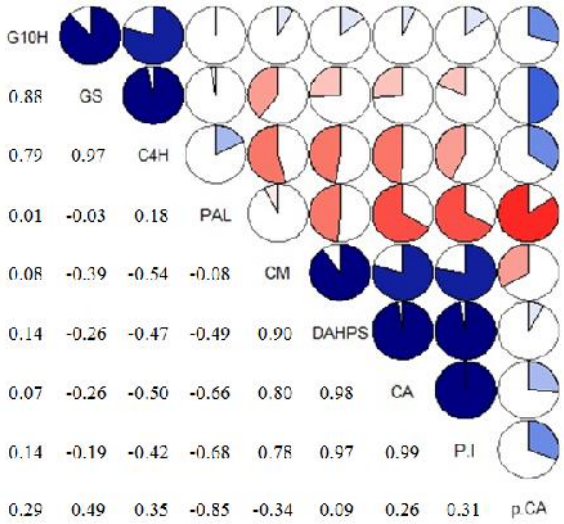

Fig. 10. Correlogram showing correlations of tested genes and metabolites data. PCC in genes and metabolites from the control, CA, CAT and CA+CAT treatment's group. The data having similar patterns are grouped together and presented in the form of pie graphs filled in proportion to the Pearson's coefficient values. Blue colored pie graphs filled clockwise indicate positive correlations while red colored pie graphs filled anti-clockwise indicate negative correlations.

Furthermore, to get insight into flux dynamics of different metabolic modules connected to picrosides biosynthesis, correlation maps were constructed between the FPKM values of selected transcripts and picrosides content among different shoots and stolons accessions of *P. kurroa*. The transcripts encoding enzymes catalyzing regulatory reactions in different metabolic pathways were selected based on their connection with picrosides biosynthesis. The details of selected transcripts with their role in picrosides production are provided in Table 2. The correlation analysis among accessions of shoots viz. PKS-1, PKS-5, PKS-4 and PKS-21 revealed positive correlations of PAL (0.66), PEPCK (0.60), DAHPS (0.92), 4CL (0.57), PK (0.03), AS (0.45), GS (0.09) and G6PDH (0.24) with P-I content while rest of the selected transcripts showed negative correlations. In contrast, the correlation analysis among accessions of stolons viz. PKST-3, PKST-5, PKST-16 and PKST-18 revealed positive correlations of PYS (0.19), DXPS (0.43), PAL (0.28), HMGR (0.94), HADH (0.13), C4H (0.60), DAHPS (0.79) and GS (0.51) with P-II content while remaining selected

transcripts showed negative correlations. These observations implied that DAHPS, PAL, PEPCK and 4CL which showed high positive correlations (>0.60) with P-I content might be considered as the key candidate genes for P-I biosynthesis. Conversely, HMGR, C4H, DAHPS and GS might play an important role in the biosynthesis of P-II in *P. kurroa*.

Table 2. Details of transcripts encoding enzymes selected for this research work and their plausible involvement in picrosides biosynthesis

Transcript encoding enzyme	Abbreviation	Function/Pathway	Flux to picrosides [Convergent (C)/ Divergent (D)]	
			P-I	P-II
1-deoxy-D-xylulose-5-phosphate synthase	DXPS	IPP & DMAPP production	C	C
3-Deoxy-D-arabinoheptulosonate 7-phosphate synthase	DAHPS	Entry step of Shikimate pathway	C	C
Hydroxymethylglutaryl-CoA reductase	HMGR	IPP production	C	C
3-hydroxyacyl CoA dehydrogenase	HADH	Benzoic acid biosynthesis	D	D
Anthranilate synthase	AS	Tryptophan biosynthesis	D	D
Tyrosine decarboxylase	TDC	Tyrosine degradation	D	D
Caffeic acid-3-O-methyltransferase	CMT	Ferulic acid production	D	C
Chalcone synthase	CHS	Flavonoids biosynthesis	D	D
Chorismate mutase	CM	Phenylalanine biosynthesis	C	C
Cinnamic acid-4-hydroxylase	C4H	p-coumaric acid production	D	C
Cinnamoyl CoA reductase	CCR	Guaiacyl lignin biosynthesis	D	D
Ferulic acid-5-hydroxylase	F5H	Syringyl lignin biosynthesis	D	D
Farnesyl pyrophosphate synthase	FPPS	Sesquiterpene biosynthesis	D	D
Geraniol synthase	GS	Monoterpene biosynthesis	C	C
Geranyl pyrophosphate synthase	GPPS	Terpene biosynthesis	C	C
Geranylgeranyl pyrophosphate synthase	GGPPS	Diterpene biosynthesis	D	D
Glucose-6-phosphate dehydrogenase	G6PDH	Pentose phosphate pathway	C	C
Hexokinase	HK	Glycolysis	C	C
Isocitrate dehydrogenase	ICDH	TCA cycle	D	D
Pytoene synthase	PYS	Carotenoid biosynthesis	D	D
Pyruvate kinase	PK	Glycolysis	C	C
Squalene synthase	SQS	Triterpene biosynthesis	D	D
4-coumarate CoA ligase	4CL	Flavonoids biosynthesis	D	D
Phenylalanine ammonia lyase	PAL	Cinnamic acid production	C	C
Phosphoenolpyruvate carboxykinase	PEPCK	Phosphoenolpyruvate production	C	C

Discussion

Elucidation of metabolic basis for P-I production

The metabolic network of picrosides production is overwhelmingly complex as multiple pathways contribute to their biosynthesis in *P. kurroa* including; primary metabolism (glycolysis, TCA cycle and pentose phosphate pathway) and secondary metabolism (S/P, MVA, MEP and monoterpene biosynthetic pathways). To elucidate the connecting links between primary and secondary metabolism, we observed changes in catalytic activities and gene expression levels of the selected glycolytic (HK and PK), TCA cycle (ICDH and MDH) enzymes and $NADP^+$-ME under differential experimental conditions viz. *P. kurroa* plants grown in field as well as in tissue culture conditions at 15°C and 25°C temperature conditions.

Interestingly, we observed that selected enzymes were positively correlated with each other as well as with the P-I content, indicated that these enzymes were likely to trigger alterations in P-I levels in *P. kurroa* shoots. However, the changes in these enzyme activities might also be due to the alterations in environmental conditions which are known to affect plants in terms of physiology, biochemistry and gene regulation pathways [33].

Therefore, to eliminate the environmental variations, we observed the metabolic basis of P-I biosynthesis in 0-40 days old shoots of *P. kurroa* grown at 15°C temperature condition in plant tissue culture chamber. The rate limiting enzymes of all the connected pathways were selected to get a more robust view of how these pathways affects P-I production and also to elucidate key steps controlling its biosynthesis in *P. kurroa* shoots. The expression of all the selected rate limiting genes remained unaltered between 0-10 days of plant growth which might indicate that already accumulated metabolites in the shoots of *P. kurroa* were responsible for initial biosynthesis of P-I. It was likely that during this period plant cells adapted to the new culture conditions as inferred from the growth and gene expression analysis. Further, increased P-I content between 10-20 days of *P. kurroa* growth might be due to elevated expression of all the selected genes during this period as compared to the 10 days stage. This statement was corroborated by the enhanced expression of G-6-PDH, DAHPS, HK, PK, DXPS, HMGR, PMK and PAL genes. The increased expression of HK, enzyme catalyzing first rate limiting step of glycolysis might produce higher levels of G-6-P, the substrate for G-6-PDH which activates the pentose phosphate pathway leading to the higher levels of erythrose-4-phosphate. The later one is the substrate for the enzyme DAHPS, considered to be rate-limiting enzyme of the S/P pathway. Further, PAL is supposed to be the entry point into P-I biosynthesis *via* the formation of CA [25]. Moreover, the increased expression of PK, another rate limiting enzyme of glycolysis, might produce higher levels of pyruvate, which is the precursor of MVA/MEP pathways [34]. The enhanced transcript levels of ISPD as compared to DXPS, HMGR and PMK genes might indicate that MEP pathway possibly played a major role in the biosynthesis of P-I. Thus, elevated transcript levels of ISPD between 10-20 days of plant growth would be associated with the supply of GPP, which is a precursor for the iridoid biosynthesis. Further, we also observed that transcripts encoding the GS and G-10-H enzymes were up-regulated between 10-20 days of plant growth which suggests their possible role in the accumulation of P-I.

Upon analyses of 30 days grown *P. kurroa* shoots, P-I content showed prominent increase and transcripts encoding HK, DXPS, ISPD, HMGR and PMK enzymes were down-regulated in comparison to 20 days grown *P. kurroa* shoots. These results indicated that HK, DXPS, ISPD, HMGR and PMK genes are likely to be involved in P-I biosynthesis for the first 20 days of plant growth and thereby might result in the accumulation of precursors required for the biosynthesis of P-I. Moreover, transcripts encoding DAHPS and G-10-H showed a highest increase at 30 days stage. In this respect, it might be inferred that DAHPS was likely to be associated with the biosynthesis of P-I possibly by activating S/P pathway, thereby hinted the production of higher concentrations of pathway intermediates known to be the precursors for P-I biosynthesis. Conversely, G-10-H is proposed to be involved in the biosynthesis of P-I via a series of hydroxylation reactions supposed to be catalysed by cytochrome p450 enzymes [25]. We can, therefore, speculate that G10H and DAHPS might act in conjunction for the increased P-I production in *P. kurroa*.

Thus, to confirm this observation, we applied metabolic flux analysis with feeding of late precursors i.e. CA and CAT alone and in combination not only to establish the route of

P-I production *in vivo* but also to determine the limiting moiety in the end metabolite. The results observed in this study showed that exogenous CAT increased P-I content when CA is not limiting indicating that addition of CAT caused rapid utilization of CA due to synergistic effect. Thus, induction of P-I production took place very rapidly after feeding with CA and CAT in combination whereas feeding with CA alone led to a small increase in P-I production (Fig. 11). This indicates that abundant supply of both CA and CAT, must exist for high rates of P-I biosynthesis to occur. Moreover, this also implies that supply of CA is limiting for the biosynthesis of P-I in *P. kurroa*. The CA serves as the branching point for formation of p-CA and P-I in *P. kurroa*. Thus, the analysis of p-CA content in CA+CAT fed shoots was performed which showed non-significant increase but CA content showed prominent elevation compared to control. One possibility for this decreased flux towards p-CA compared to P-I is that the exogenous supply of both CA and CAT in combination might increase the activity of probable acyltransferase catalysing the esterification step between CA and CAT to produce P-I. It should be noted that we have not detected the activity of this enzyme, since this probable acyltransferase is still to be identified. Further, the decreased transcript level of C4H in CA+CAT fed shoots might also support the non-significant increase in p-CA production over control. Furthermore, the rapid utilization of exogenous CA for P-I production in CA+CAT fed shoots appears to induce the cells to synthesize more CA as indicated by high CA content. It might direct the flux of S/P pathway through to the prephenate synthesis step leading to increased Phe availability. This statement was corroborated by enhanced expression of genes encoding DAHPS and CM; enzymes considered to be rate limiting along with PAL for the S/P pathway [16]. CA has been proposed to feedback inhibit PAL activity. Our results showed significant increase in PAL activity which indicates that the rapid utilization of CA might have a de-inhibitory effect on the activity of PAL enzyme (Fig. 11). However, CA+CAT feeding decreased the transcript level of gene encoding PAL. This implies that exogenously supplied CA+CAT exerted both coarse and fine controls to the reaction catalyzed by PAL enzyme. As a whole there are convincing evidences that S/P pathway stimulate flux during combined augmentation of CA and CAT levels in *P. kurroa*. Moreover, the analyses of CA fed shoots revealed that the exogenous feeding of CA alone directed the flux both towards p-CA and P-I compared to CA+CAT fed shoots possibly due to the limited CAT supply. Apparently, less utilization of CA pool compared to CA+CAT fed shoots appears to inhibit synthesis of endogenous CA as indicated by non-significant increase in CA content compared to control. This statement was in agreement with the results observed which showed significant reduction in PAL activity and gene expression indicating the feedback inhibition of PAL enzyme by both coarse and fine controls. Thus, it can be concluded that CA and CAT are found to be stimulating enhanced P-I production whereas their individual application caused feedback inhibition and limits the production of P-I.

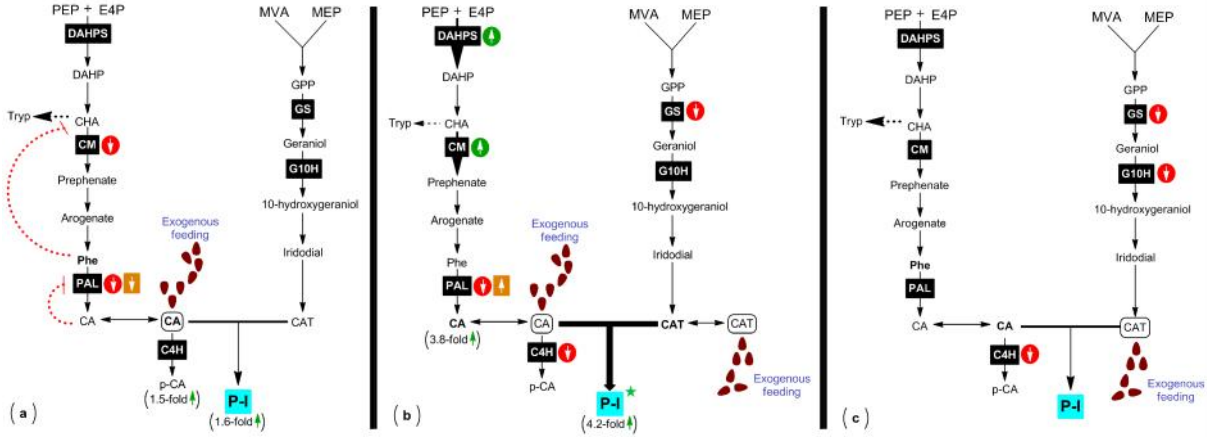

Fig. 11. Cascades depicting influence of different treatments on the fluxes through S/P and iridoid pathways; (a) CA, (b) CA+CAT and, (c) CAT. The symbols were added and structures were coded with different colors to highlight the effects occurring on the biosynthesis of P-I under different treatments. Gene expressions were highlighted by using the green circle with arrow pointing up shows up-regulation while red circle with arrow pointing down shows down-regulation. Orange colored box with arrow pointing up and down indicate up-regulation and down-regulation of PAL enzyme, respectively. Red colored loop indicate feedback inhibition effect. Bold arrows indicate the up-regulation of respective step. Green colored star indicate high significant increase.

Elucidation of metabolic basis for P-II production

To investigate the metabolic basis of P-II biosynthesis, we have employed a strategy utilizing natural genetic diversity existing for the production of P-II among *P. kurroa* accessions collected from different geographic locations of North-Western Himalayas, India. The analysis of stolon tissues from different *P. kurroa* accessions revealed prominent increase in P-II content upon reduction in P-I level indicating that both P-I and P-II biosynthesis skewed from a common metabolic node. It is likely since VA, the immediate precursor of P-II; is supposed to be formed from either PA or FA, both are derived from S/P pathway which also produces CA, the immediate biosynthetic precursor of P-I. Therefore, it is crucial to monitor dynamic profiles of intermediate metabolites in S/P pathway to get deep insight for metabolic switches of P-II biosynthesis. To address this, we have analysed stolon tissues of four *P. kurroa* accessions with varying P-II content and revealed that VA content increased among high P-II content stolon tissues (PKST-3 and PKST-5) compared to low P-II content stolons (PKST-16 and PKST-18) which established that VA is associated with P-II biosynthesis. Further, the analysis of CA and p-CA metabolites contents in selected stolon tissues revealed that 87% CA was converted to p-CA in PKST-5 (P-1, 0.08%; P-II, 2.19%), 44.4% in PKST-3 (P-1, 0.17%; P-II, 2.65%), 21.1% in PKST-16 (P-1, 1.05%; P-II, 1.52%) and 8.2% in PKST-18 (P-1, 1.32%; P-II, 1.36%). This implies that with increase in the P-I content, the flux of S/P pathway limits through to the CA step to p-CA while increase in the P-II content directs the flux of S/P pathway through to the CA to p-CA leading to the enhanced P-II production in *P. kurroa*. This statement is also supported by comparative transcriptome analysis of selected stolon tissues which showed high positive correlation of gene encoding C4H (0.60) with P-II content compared to gene encoding PAL enzyme which showed PCC of 0.28 with P-II content. The C4H catalyzes the conversion of CA to p-CA while PAL catalyzes the conversion of phenylalanine to CA. We have thus, hypothesised that CA is the common

metabolic node between P-I and P-II biosynthesis in *P. kurroa* rather than 3-dehydroshikimate which serves as the branch point between PA and shikimate production; the metabolites also supposed to be the common nodes for P-I and P-II biosynthesis [25].

The analysis of FA, however, did not show significant variations among stolon tissues but increased VA content was observed in stolons having high P-II content compared to low P-II content stolons. Keeping in view, FA is a canonical intermediate metabolite in the biosynthesis of guaiacyl- and syringyl lignins in addition to its proposed role in VA production, the observed results might indicate that flux of FA is directed towards both VA and P-II in PKST-3 and PKST-5, whereas maximum flux of FA might deviate to lignin biosynthesis in PKST-16 and PKST-18. This statement is in agreement with correlation map constructed between P-II content and transcripts abundance values (FPKM) which revealed negative correlation of gene encoding CMT with P-II content (-0.63) followed by a strong positive correlation of CMT through a PCC value of 0.82 with F5H, an enzyme that catalyzes the conversion of FA to 5-hydroxy ferulic acid, which represents as a precursor for syringyl lignin biosynthesis [35]. Consequently, it is apparent that up-regulated transcript level of CMT; an enzyme catalyzing the conversion of caffeic acid to FA accompanied by F5H, might be linked to the activation of lignin biosynthesis in PKST-16 and PKST-18.

Previous studies have reported that shoots of *P. kurroa* are independent tissues for P-I production. Nevertheless, current study established stolons of *P. kurroa* as autonomous biosynthetic machinery for P-I and P-II, both share a common biosynthetic pathway, it is inspiring to comprehend the negligence of P-II biosynthesis in *P. kurroa* shoots. The analysis of shoot tissues of four *P. kurroa* accessions for CA and p-CA revealed that increased P-I production limits flux of CA towards p-CA biosynthesis. In contrast, the analysis of FA revealed slight variation between the shoots accessions and also showed a high positive correlation by PCC of 0.85 with p-CA. However, C4H and CHS showed a strong positive correlation with PCC of 0.90 compared to PCC of 0.23 between C4H and CMT. CHS catalyzes the formation of chalcone which acts as a starting metabolite for flavonoids biosynthesis. Therefore, this finding underscores that phenylpropanoid pathway might allocate the flux of p-CA to produce both FA and flavonoids in *P. kurroa* shoots. Interestingly, negligible levels of VA were observed in all the selected shoot tissues which implies that P-II biosynthesis arrests in the downstream steps of FA, which possibly limits the VA supply.

Therefore, p-CA, FA and PA were exogenously applied along with mixture of VA and catalpol in tissue culture conditions which revealed increased VA content in FA fed shoots compared to control. This observation further ascertained the association of FA with VA production. Moreover, increased VA content in VA+CAT fed shoots over control might indicate it's accumulation due to exogenous application. This was also supported by the absence of VA content in the MS media left after the collection of VA+CAT fed shoots. Moreover, the P-II content analysis revealed its minor detection in VA+CAT fed shoots which indicate that exogenous application of VA+CAT, might stimulate its production in *P. kurroa* shoots (Fig. 12). Therefore, different concentrations of VA+CAT were further tested but unfortunately, we did not observe significant increment in P-II content among different VA+CAT fed shoots which is possibly due to low activity of a probable acyltransferase that catalyses the esterification of VA and CAT to produce P-II. However, we have not observed the activity of probable acyltransferase as it is not discovered yet. It is striking that P-II was not taken up by the *P. kurroa* plants upon its exogenous introduction which was clearly

demonstrated from the negligible level of P-II observed in shoots fed with P-II whereas its substantial content was detected in the MS media left after the collection of P-II fed shoots. This finding suggests that *P. kurroa* plants are unable to take P-II in its ready form and subsequently they are dependent on its endogenous production.

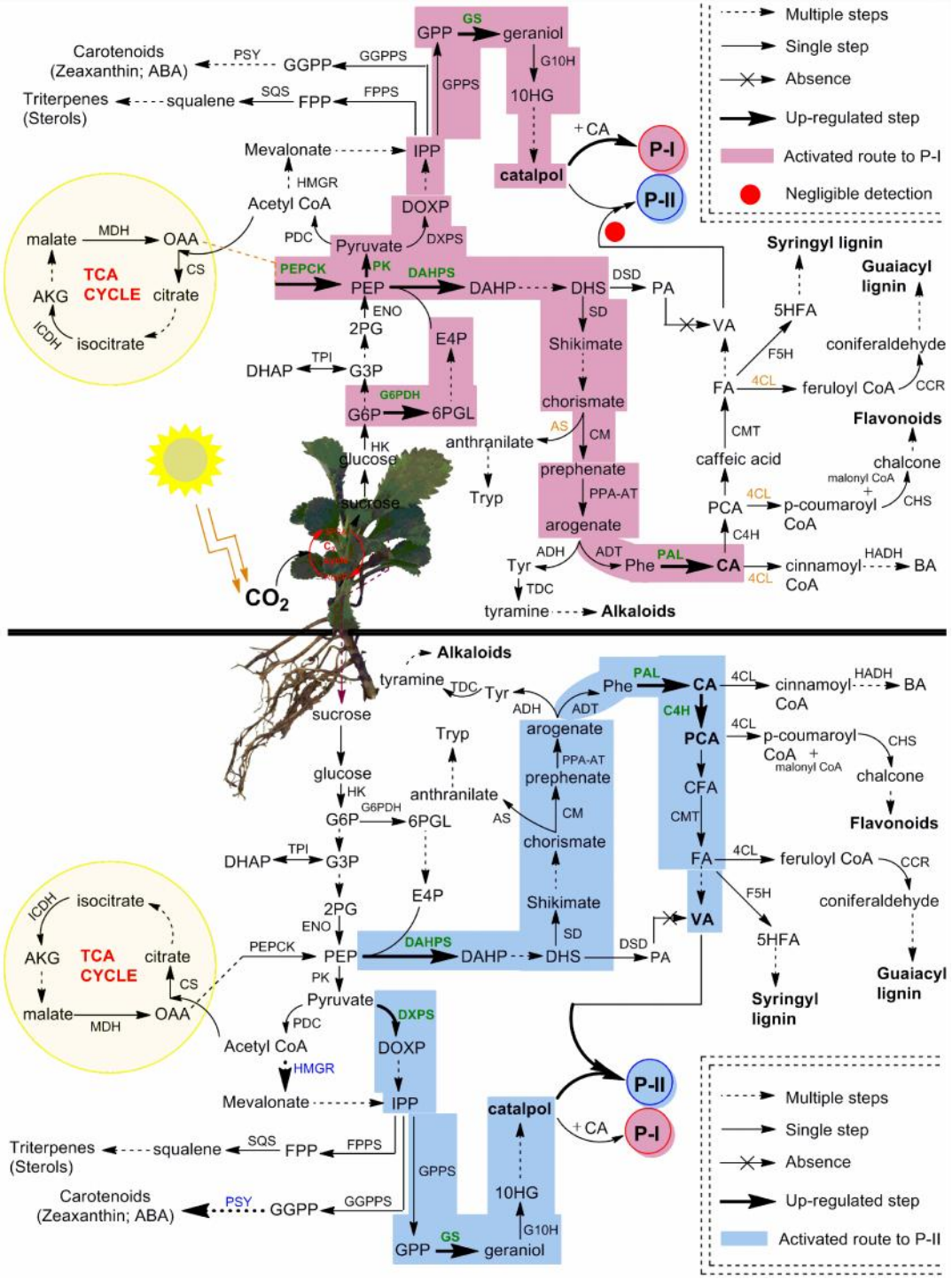

Fig. 12. Complete framework of metabolic network depicted P-I and P-II biosynthesis in different compartments of *P. kurroa*. The established routes of P-I and P-II production were presented with different colors to highlight the modulations in shoots and stolons tissues of *P. kurroa*. Up-regulated gene expressions were highlighted with bold and green color.

Conclusions and future prospects

The findings of this research work shed light on metabolic modulations underlying the biosynthesis of P-I and P-II in *P. kurroa*. It offers convincing evidences that independent mechanisms control the biosynthesis of P-I and P-II in both compartments of *P. kurroa* i.e. shoots and stolons. The intermediates of shikimate/phenylpropanoid pathway produced in stolons guided the flux towards P-II biosynthesis via degradation of FA to produce VA, while deviate from the non-canonical view of P-II biosynthesis in shoot tissues of *P. kurroa*. Moreover, CA is found to be the limiting moiety for P-I production and supplementing CA+CAT is found to be activating both S/P and iridoid pathways for enhanced P-I production whereas their individual application caused feedback inhibition and limits the production of P-I. As a whole in the face of such a complex biosynthetic architecture, one may ask what strategy we should focus on for biosynthetic engineering of P-I in *P. kurroa*. Indeed, we argue that multi-step engineering for augmenting both CA and CAT by exploitation of DAHPS, CM, PAL, GS and G10H catalyzed steps is more prosaic. Finally, we have illustrated the basis of P-II negligence in shoot compartment that provides impetus for the future investigation of an enzyme catalyzing the conversion of VA and CAT to produce P-II, a task that can rewrite the P-II production in shoots of *P. kurroa*.

References

[1] Pandit S, Shitiz K, Sood H, Chauhan RS (2013) Differential biosynthesis and accumulation of picrosides in an endangered medicinal herb *Picrorhiza kurroa*. J Plant Biochem Biotechnol 22(3):335–342.

[2] Kumar V, Chauhan RS, Tandon C (2016) Biosynthesis and therapeutic implications of iridoid glycosides from Picrorhiza genus: the road ahead. J Plant Biochem Biotechnol (In Press). DOI: 10.1007/s13562-016-0364-8

[3] Comu FM, Kilic Y, Ozer A, Kirisci M, Dursun AD, Tatar T, Zor MH, Kartal H, Kucuk A, Boyunaga H, Arslan M (2016) Effect of picroside II on erythrocyte deformability and lipid peroxidation in rats subjected to hind limb ischemia reperfusion injury. Drug Des Devel Ther 10:927-931.

[4] Choi J, Choi BK, Kim JS, Lee JW, Park HA, Ryu HW, Lee SU, Hwang KW, Yun WK, Kim HC, Ahn KS, Oh SR, Lee HJ (2016) Picroside II attenuates airway inflammation by down-regulating the transcription factor GATA3 and Th2-related cytokines in a mouse model of HDM-induced allergic asthma. PLoS One 11:e0167098.

[5] Wang LEI, Liu X, Chen HUI, Chen Z, Weng X, Qiu TAO, Liu LIN (2015) Effect of picroside II on apoptosis induced by renal ischemia/reperfusion injury in rats. Exp Ther Med 9:817-822.

[6] Guo Y, Xu X, Li Q, Li Z, Du F (2010) Anti-inflammation effects of picroside 2 in cerebral ischemic injury rats. Behav Brain Funct 6:43.

[7] Li Q, Li Z, Xu XY, Guo YL, Du F (2010) Neuroprotective properties of picroside II in a rat model of focal cerebral ischemia. Int J Mol Sci 11:4580-4590.

[8] Liu G, Zhao L, Wang T, Zhang M, Pei H (2014) Optimal therapeutic dose and time window of picroside II in cerebral ischemic injury. Neural Regen Res 9:1437-1445.

[9] Pei H, Su X, Zhao L, Li H, Guo Y, Zhang M, Xin H (2012) Primary study for the therapeutic dose and time window of picroside II in treating cerebral ischemic injury in rats. Int J Mol Sci 13:2551-2562.

[10] Wang T, Zhai L, Guo Y, Pei H, Zhang M (2015) Picroside II has a neuroprotective effect by inhibiting ERK1/2 activation after cerebral ischemic injury in rats. Clin Exp Pharmacol Physiol (In Press). DOI: 10.1111/1440-1681.12445

[11] Zhao L, Guo Y, Ji X, Zhang M (2014) The neuroprotective effect of picroside II via regulating the expression of myelin basic protein after cerebral ischemia injury in rats. BMC Neurosci 15:25.

[12] Gao H, Zhou YW (2005) Inhibitory effect of picroside II on hepatocyte apoptosis. Acta Pharmacol Sin 26:729-736.

[13] Gao H, Zhou YW (2005) Anti-lipid peroxidation and protection of liver mitochondria against injuries by picroside II. World J Gastroenterol 11:3671-3674.

[14] Meng FJ, Hou ZW, Li Y, Yang Y, Yu B (2012) The protective effect of picroside II against hypoxia/reoxygenation injury in neonatal rat cardiomyocytes. Pharm Biol 50:1226-1232.

[15] Meng FJ, Jiao SM, Yu B (2012) Picroside II protects cardiomyocytes from hypoxia/reoxygenation-induced apoptosis by activating the PI3K/Akt and CREB pathways. Int J Mol Med 30:263-270.

[16] Wu N, Li W, Shu W, Jia D (2014) Protective effect of picroside II on myocardial ischemia reperfusion injury in rats. Drug Des Devel Ther 8:545-554.

[17] Dwivedi YRR, Garg NK, Dhawan BN (1992) Picroliv and its components kutkoside and P-I protect liver against galactosamine induced damage in rats. Pharmacol Toxicol 71:383-387.

[18] Rathee D, Thanki M, Bhuva S, Anandjiwala S, Agrawal R (2013) Iridoid glycosides-Kutkin, Picroside I, and Kutkoside from *Picrorrhiza kurroa* Benth inhibits the invasion and migration of MCF-7 breast cancer cells through the down regulation of matrix metalloproteinases: 1st Cancer Update. Arabian J Chem 6:49-58.

[19] Li P, Matsunaga K, Yamakuni T, Ohizumi Y (2000) Potentiation of nerve growth factor-action by picrosides I and II, natural iridoids, in PC12D cells. Eur J Pharmacol 406:203-208.

[20] Li P, Matsunaga K, Yamakuni T, Ohizumi Y (2002) Picrosides I and II, selective enhancers of the mitogen-activated protein kinase-dependent signaling pathway in the action of neuritogenic substances on PC12D cells. Life Sci 71:1821-1835.

[21] Sood H, Chauhan RS (2010) Biosynthesis and accumulation of a medicinal compound, picroside-I, in cultures of *Picrorhiza kurroa* Royle ex Benth. Plant Cell Tiss Org Cult 100:113–117.

[22] Sharma N, Kumar V, Chauhan RS, Sood H (2016) Modulation of picroside-I biosynthesis in grown elicited shoots of *Picrorhiza kurroa* in vitro. J Plant Growth Regul 35(4):965-973.

[23] Kumar V, Sood H, Sharma M, Chauhan RS (2013) A proposed biosynthetic pathway of picrosides linked through the detection of biochemical intermediates in the endangered medicinal herb *Picrorhiza kurroa*. Phytochem Anal 24(6):598–602.

[24] Pandit S, Shitiz K, Sood H, Naik PK, Chauhan RS (2013) Expression pattern of fifteen genes of non-mevalonate (MEP) and mevalonate (MVA) pathways in different tissues of endangered medicinal herb *Picrorhiza kurroa* with respect to picrosides content. Mol Biol Rep 40(2):1053–1063.

[25] Shitiz K, Sharma N, Pal T, Sood H, Chauhan RS (2015) NGS transcriptomes and enzyme inhibitors unravel complexity of picrosides biosynthesis in *Picrorhiza kurroa* Royle ex. Benth. PLoS ONE 10(12):e0144546.
[26] Bourgaud F, Gravot A, Milesi S, Gontier E (2001) Production of plant secondary metabolites: a historical perspective. Plant Sci 161:839–851.
[27] Whitmer S, Canel C, Hallard D, Goncalves C, Verpoorte R (1998) Influence of precursor availability on alkaloid accumulation by transgenic cell line of *Catharanthus roseus*. Plant Physiol 116:853–857.
[28] Gahlan P, Singh HR, Shankar R, Sharma N, Kumari A, Chawla V, Ahuja PS, Kumar S (2012) *De novo* sequencing and characterization of *Picrorhiza kurrooa* transcriptome at two temperatures showed major transcriptome adjustments. BMC Genom 13:126.
[29] Nour V, Trandafir I, Cosmulescu S (2012) HPLC determination of phenolic acids, flavonoids and Juglone in Walnut leaves. J Chromatogr Sci 51(9):883-890.
[30] Pal T, Malhotra N, Chanumolu S, Chauhan RS **(**2015) Next-generation sequencing (NGS) transcriptomes reveal association of multiple genes and pathways contributing to secondary metabolites accumulation in tuberous roots of *Aconitum heterophyllum* Wall. Planta 242(1):239-58.
[31] Quinlan AR, Hall IM (2010) BEDTools: a flexible suite of utilities for comparing genomic features. Bioinformatics 26(6):841–842.
[32] Li H, Handsaker B, Wysoker A, Fennell T, Ruan J, Homer N, Marth G, Abecasis G, Durbin R (2009) The sequence alignment/map format and SAMtools. Bioinformatics 25(16):2078–2079.
[33] Bita CE, Gerats T (2013) Plant tolerance to high temperature in a changing environment: scientific fundamentals and production of heat stress-tolerant crops. Front Plant Sci 4:273.
[34] Lange BM, Rujan T, Martin W, Croteau R (2000) Isoprenoid biosynthesis: the evolution of two ancient and distinct pathways across genomes. Proc Natl Acad Sci 97(24):13172–13177.
[35] Wagner A, Tobimatsu Y, Phillips L, Flint H, Geddes B, Lu F, Ralph J (2015) Syringyl lignin production in conifers: Proof of concept in a Pine tracheary element system. Proc Natl Acad Sci 112(19):6218-6223.

LIST OF PUBLICATIONS

1. **Kumar V,** Bansal A, Chauhan RS (2016) Modular design of picroside-II biosynthesis deciphered through NGS transcriptomes and metabolic intermediates analysis in naturally variant chemotypes of a medicinal herb, *Picrorhiza kurroa*. Plant Cell Environ (Communicated). Manuscript ID: PCE-16-0996. **(IF: 6.16; SCOPUS)**
2. **Kumar V**, Sharma N, Sood H, Chauhan RS (2016) Exogenous feeding of immediate precursors reveals synergistic effect on picroside-I biosynthesis in shoot cultures of *Picrorhiza kurroa* Royle ex Benth. Sci Rep 6:29750. **(IF: 5.22; SCOPUS)**
3. **Kumar V**, Chauhan RS, Tandon C (2016) Biosynthesis and therapeutic implications of Iridoid glycosides from Picrorhiza genus: the road ahead. J Plant Biochem Biotechnol (In press). DOI: 10.1007/s13562-016-0364-8 **(IF: 1.35; SCOPUS)**

4. **Kumar V,** Shitiz K, Chauhan RS, Sood H, Tandon C (2016) Tracking dynamics of enzyme activities and their gene expression in *Picrorhiza kurroa* with respect to picroside accumulation. J Plant Biochem Biotechnol 25(2):125-132. **(IF: 1.35; SCOPUS)**
5. **Kumar V,** Sharma N, Shitiz K, Singh TR, Tandon C, Sood H, Chauhan RS (2015) An insight into conflux of metabolic traffic leading to picroside-I biosynthesis by tracking molecular time course changes in a medicinal herb, *Picrorhiza kurroa*. Plant Cell Tiss Org Cult 123(2):435-441. **(IF: 2.39; SCOPUS)**
6. **Kumar V**, Kumar V, Chauhan RS, Sood H, Tandon C (2015) Cost effective quantification of picrosides in *Picrorhiza kurroa* by employing response surface methodology using HPLC-UV. J Plant Biochem Biotechnol 24(4):376-384. **(IF: 1.35; SCOPUS)**
7. Sharma N, **Kumar V,** Chauhan RS and Sood H (2016) Modulation of picroside-I biosynthesis in grown elicited shoots of *Picrorhiza kurroa* in vitro. J Plant Growth Regul 35(4):965-973. **(IF: 2.16; SCOPUS)**

CONFERENCES/WORKSHOPS

1. **Kumar V,** Chauhan RS (2016) **Oral Presentation** on "Biosynthetic Pathways Discovery for Major Medicinal Compounds in Endangered Medicinal Herbs of North-Western Himalayas" at International conference on "*Biodiversity: Current Scenario and Future Strategies*" sponsored by "**State Council for Science, Technology and Environment Himachal Pradesh**" held at St. Bede's College, Shimla, October 6-8.
2. **Kumar V,** Chauhan RS (2016) Presented a poster on 'Exogenous feeding of cinnamic acid and catalpol directs metabolic flux towards Picroside-I biosynthesis in a medicinal herb, *Picrorhiza kurroa* Royle Ex Benth' at **INDO-US** Workshop on "Cell Factories", held at IIT Bombay, Mumbai, March 18-20.
3. Participated in an **ICMR sponsored** National Workshop-cum-Training Programme on "Standardization of Medicinal Plants and their Products", held at Shoolini University, Solan, March 22-24, 2015.
4. **Kumar V**, Chauhan RS, Tandon C (2013). Presented a poster on 'Optimization of picrosides extraction from *Picrorhiza kurroa* using HPLC-UV by employing response surface methodology' at 7th Annual Convention of ABAP and International Conference on Plant Biotechnology, Molecular Medicine and Human Health, held at Delhi University (South Campus), New Delhi, October 18-20.

ACKNOWLWDGEMENTS

I want to thank Department of Biotechnology, Ministry of Science and Technology, Government of India for providing financial support to RSC in the form of a Programme Support on high-value medicinal plants under Centres of Excellence. We are also thankful to the Himalayan Forest Research Institute (HFRI), Panthaghati, Shimla, India for providing authenticated plant material of P. kurroa.